

Disorder Effects in the Bipolaron System Ti_4O_7 Studied by Photoemission Spectroscopy

K. Kobayashi*, T. Susaki, A. Fujimori^a, T. Tonogai^b, and H. Takagi^c

Department of Physics, University of Tokyo, Bunkyo-ku, Tokyo, 113-0033, Japan

^a*Department of Physics and Department of Complexity Science and Engineering,
University of Tokyo, Bunkyo-ku, Tokyo 113-0033, Japan*

^b*Department of Applied Physics, University of Tokyo, Bunkyo-ku, Tokyo 113-0033, Japan*

^c*Department of Applied Chemistry and Department of Advanced Materials Science,
University of Tokyo, Bunkyo-ku, Tokyo 113-0033, Japan*

(August 30, 1999)

We have performed a photoemission study of Ti_4O_7 around its two transition temperatures so as to cover the metallic, high-temperature insulating (bipolaron-liquid), and low-temperature insulating (bipolaron-crystal) phases. While the spectra of the low-temperature insulating phase show a finite gap at the Fermi level, the spectra of the high-temperature insulating phase are gapless, which is interpreted as a soft Coulomb gap due to dynamical disorder. We suggest that the spectra of the high-temperature disordered phase of Fe_3O_4 , which exhibits a charge order-disorder transition (Verwey transition), can be interpreted in terms of a Coulomb gap.

PACS numbers: 71.23.-k, 71.30.+h, 72.80.Ga, 79.60.-i

Since Mott [1] proposed the idea of variable-range hopping and minimum metallic conductivity for disordered systems and Anderson [2] raised the concept of localization due to disorder, physical properties of disordered solids have been extensively studied. Influence of Coulomb interaction on the electronic density of states (DOS) near the Fermi level (E_F) of disordered systems is one of the most fundamental issues to be clarified. Efros and Shklovskii [3] proposed that in disordered insulators long-range Coulomb interaction opens a soft Coulomb gap (SCG), whose DOS is proportional to $(E - E_F)^2$. So far, there have been tunneling spectroscopic confirmations of the SCG in some disordered systems such as doped semiconductors [4]. Davies and Franz [5] pointed out the possibility of an SCG opening in the photoemission spectra of $\text{Na}_x\text{Ta}_y\text{W}_{1-y}\text{O}_3$ [6], but the experiments did not have sufficient energy resolution to critically address this problem. Another important issue is how short-range order (SRO) affects DOS near E_F , that is, how the electronic structure evolves when a charge ordering develops from disorder to SRO to long-range order.

Ti_4O_7 is a suitable system to study the above problems: It undergoes successive phase transitions with decreasing temperature from a metal to a charge-ordered insulator via an insulator with SRO [7]. It is a system with nominally 0.5 $3d$ electron per Ti, allowing two possible valence states of Ti^{3+} ($3d^1$) and Ti^{4+} ($3d^0$), and attracted particular attention in 1970's as a system where bipolarons, or singlet pairs of two polarons, are formed in real space [7–9]. Above $T_{MI} = 154$ K, the system is in the metallic (M) phase and the Ti valence is believed to be uniform $3.5+$ as shown in Fig. 1 (a). That is, the electrical resistivity $\rho(T)$ is metallic with Pauli-paramagnetic $\chi(T)$. With decreasing temperature, sin-

glet Ti^{3+} - Ti^{3+} pairs, namely bipolarons, are formed, resulting in the metal-to-insulator transition at T_{MI} with a steep increase in $\rho(T)$ by three orders of magnitude. At the same time, $\chi(T)$ almost vanishes, reflecting the formation of the singlet bipolarons. We refer to this phase as the high-temperature insulating (HI) phase. Because the bipolarons are dynamically disordered in this phase as has been established by EPR studies [10], the HI phase may be called a bipolaron liquid. Subsequently, bipolarons become ordered below $T_{II} \sim 140$ K as shown in Fig. 1 (a), with a further rise in $\rho(T)$ by three orders of magnitude while $\chi(T)$ remains unaffected. We refer to this phase as the low-temperature insulating (LI) phase. The transition from the liquid to the crystal of bipolarons is a kind of Verwey transition [11,12] and the bipolaron-liquid formation in the HI phase is a kind of a SRO of charge carriers. The Verwey transition [13] was originally found for Fe_3O_4 at $T_V \simeq 120$ K. Analogous to Ti_4O_7 , Fe_3O_4 has two possible valence states of Fe^{2+} and Fe^{3+} which are ordered below T_V and are disordered above T_V , leading to the characteristic jump in the electrical resistivity.

In this Letter, we have studied the single-particle excitation spectra of the three phases of Ti_4O_7 by means of photoemission spectroscopy (PES) with high energy resolution. To add to the variation of the electronic structure of Ti_4O_7 as a function of temperature across T_{MI} and T_{II} , we focus on general aspects of the single-particle excitation spectra of dynamically disordered systems and then made comparison with the PES result of Fe_3O_4 [14].

Single crystals of Ti_4O_7 were grown by the vapor transport method [15]. PES measurements were performed using an OMICRON hemi-spherical analyzer and a He lamp (He I: $h\nu = 21.2$ eV). The energy calibration and the estimation of the instrumental resolution were done

by measuring the Fermi edge of Au evaporated on the sample. The energy resolution was set ~ 50 meV. Samples were cleaved *in situ*. This always gave an irregular surface, an assembly of randomly orientated small facets. As the analyzer had an acceptance angle of $\pm 8^\circ$, the obtained spectra can be regarded as angle-integrated PES spectra. The measurement temperature was controlled within the accuracy of ± 0.2 K. The base pressure in the spectrometer was less than 1×10^{-10} Torr. Below, we show results reproducible for several cleaves and obtained within a few hours after cleavage.

The position and the width of the O $2p$ band (not shown) show almost no temperature dependence across the two phase transitions as in the previous photoemission study [16]. In contrast, the PES spectra in the Ti $3d$ band region show strong temperature dependence as shown in Fig. 1 (b), being consistent with the previous results for the M and LI phases with a lower energy resolution [16]. Here, the sample was first cooled and then heated as indicated in the figure, so as to cross twice each transition temperature. Two observations are remarked. First, as superimposed in the bottom panel, there are three kinds of spectra, which reflect the electronic structure of the M, HI, and LI phases of Ti_4O_7 as discussed below. Second, the 142 K spectra show different spectral lineshapes between cooling and heating due to thermal hysteresis between the HI and LI phases, as has been observed in the electrical resistivity, thermopower [7], and EPR measurements [10]. In Fig. 1 (c), we have plotted the temperature dependence of the integrated PES intensity within 0.5 eV of E_F normalized to the intensity integrated from E_F to binding energy $E_B = 1$ eV. This hysteretic behavior was reproducible for several thermal cyclings across T_{MI} and T_{HI} .

Let us discuss the spectra of each phase in more detail. As shown in Fig. 1 (d), M-phase spectra show a weak but finite Fermi edge, reflecting its metallic nature. The spectrum shows a broad maximum centered at $E_B = 0.75$ eV, around which most of spectral weight is distributed. A similar broad feature has been observed at $E_B \sim 1$ –1.5 eV in the spectra of three-dimensional titanium and vanadium oxides with $3d^1$ configuration, LaTiO_3 and YTiO_3 [17], and has been interpreted as the incoherent part of the spectral function accompanying the coherent quasi-particle excitations around E_F . The coherent part in Ti_4O_7 is hardly separable from the incoherent part because of their strong overlap, leading to the pseudo-gap-like behavior at E_F . This implies that the M phase of Ti_4O_7 is a strongly correlated metal, where the motion of conduction electrons is largely incoherent, resulting in the weak coherent part. In going from the M to the LI phase, the incoherent peak at $E_B = 0.75$ eV becomes sharper and a clear gap of order ~ 0.1 eV is opened as seen in Fig. 1 (d). The gap opening is attributed to the bipolaron ordering in this phase. The HI-phase spectra take an intermediate lineshape between the LI and

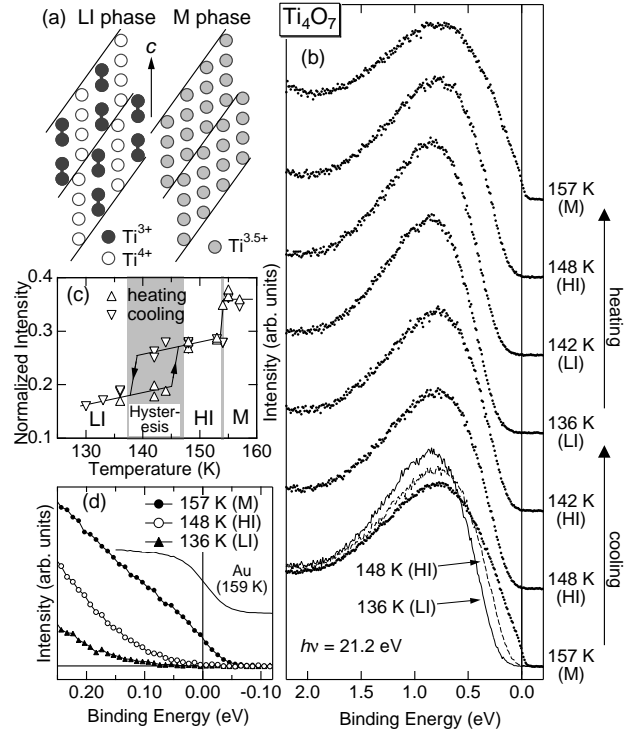


FIG. 1. (a) Schematic crystal structures of Ti_4O_7 which show only the chains parallel to the pseudo-rutile c -axis truncated by shear planes indicated by thick lines [8]. In the LI phase, the bipolarons are ordered. In the M phase, all the Ti sites have a uniform valence of 3.5+. (b) PES spectra of Ti_4O_7 taken by varying the temperature from the bottom to the top. (c) Normalized PES intensity near E_F (see text). The solid line is guide to the eye. (d) The M-, HI-, and LI-phase spectra around E_F plotted on an expanded scale.

M phases: The 0.75 eV peak is somewhat broader than in the LI phase. The spectra show neither a Fermi edge nor a real gap. Indeed, the PES intensity vanishes only at $E_B = 0.0$ eV as shown in Fig. 1 (d). Figure 2 (a) shows the same spectra plotted against $E_B^2 \text{sgn}(E_B)$. The Fermi edge in the M-phase spectra is now clearer while the LI spectra, which show a “hard gap”, are concave around E_F . Most remarkably, the HI-phase spectra form an almost straight line from $E_B^2 = 0.00$ to ~ 0.08 eV² ($0.0 \leq E_B \lesssim 0.3$ eV), meaning that the spectra show a power-law behavior with the exponent of ~ 2 .

To be more quantitative, we have performed a lineshape analysis for the LI- and HI-phase spectra taking the experimental resolution into account. The lineshape was assumed to be of the form $I(E_B, T) = I_0(E_B, T) + I_{bg}(E_B)$, where $I_0(E_B, T)$ is the intrinsic part expressed by $I_0(E_B, T) = a_2 E_B^2 f(E_B, T)$. $f(E_B, T) = [\exp(-E_B/k_B T) + 1]^{-1}$ is the Fermi-Dirac distribution function at T although the finite-temperature effect due to $f(E_B, T)$ is negligibly small because $I_0(0, T) = 0$. $I_{bg}(E_B) = b_0$ represents a constant background of the

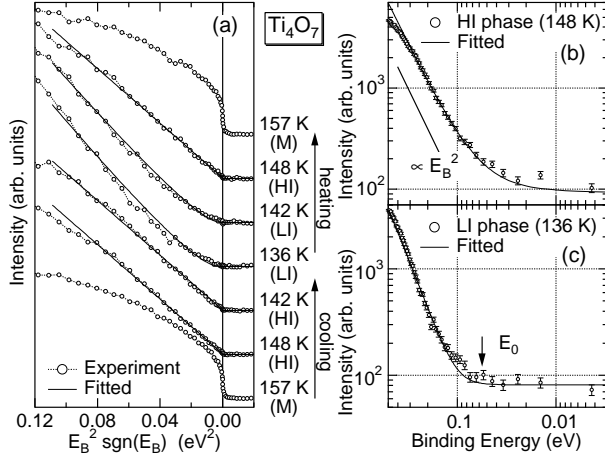


FIG. 2. (a) PES spectra of Ti_4O_7 plotted against $E_B^2 \text{sgn}(E_B)$ with the fitted curves. The experimental spectrum and the fitted curve plotted on the log-log scale for the HI phase (b) and the LI phase (c).

PES spectra. For the LI phase, in order to represent the finite gap, we assumed $I_0(E_B, T) = a_2(E_B - E_0)^2 \theta(E_B - E_0)$, where $\theta(x)$ is a step function and E_0 was allowed to take a finite positive value. The instrumental resolution was included through the convolution of $I(E_B, T)$ with a Gaussian of FWHM 50 meV. a_2 and b_0 were treated as adjustable parameters. As shown in Fig. 2 (a), the result of the fitting is satisfactory, especially for the HI-phase spectra for $-0.1 \leq E_B \leq 0.3$ eV. One HI-phase spectrum is shown in Fig. 2 (b) on the log-log scale to emphasize the E_B^2 dependence and the excellent fit for small E_B . This makes a clear contrast to the LI-phase spectrum shown in Fig. 2 (c), which shows a finite gap of E_0 .

We propose that the above behavior of the HI phase can be explained as an SCG in the DOS, $N(E_B) = \frac{3}{\pi}(\frac{\kappa}{e^2})^3 E_B^2$ [3], where κ is the dielectric constant. For Ti_4O_7 , the magnitude of the SCG $\Delta_C = e^3(N_0/\kappa^3)^{1/2}$, where N_0 is the noninteracting DOS at E_F , is estimated to be ~ 0.2 eV if we take $N_0 \sim 0.01 \text{ eV}^{-1} \text{ \AA}^{-3}$ from the free-electron-like DOS around E_F and $\kappa \sim 10$. As the estimated Δ_C and the observed soft gap have the same order of magnitude, we may conclude that the HI-phase spectra are consistent with the opening of an SCG. Here, it should be noted that, even if there exists substantial SRO, i. e., bipolaron-liquid formation, in the HI phase of Ti_4O_7 the system is sufficiently disordered over long distance for an SCG to appear around E_F . That is, the length scale of the SRO, which is equal to the Ti-Ti distance $\sim 3 \text{ \AA}$ [8], is sufficiently shorter than the critical distance $R_C \sim e^2/\kappa\Delta_C \sim 8 \text{ \AA}$ for the SCG to survive. The SRO would be reflected on high-energy spectral features, e. g., the sharpening of the $E_B = 0.75$ eV peak in the HI phase. Experimentally, an SCG was observed in tunneling spectroscopy measurements of the doped semicon-

ductor Si:B [4], whose gap was as small as 0.75 meV due to low N_0 . As for PES measurements, besides the aforementioned $\text{Na}_x\text{Ta}_y\text{W}_{1-y}\text{O}_3$, possible existence of SCG in Ti_4O_7 and Fe_3O_4 was suggested [5], while no quantitative analysis on the experimental spectra has been performed so far. In this sense, the present result $I \propto E_B^2$ for the HI phase of Ti_4O_7 is the first clear indication of an SCG using PES. Since our measurements were performed on cleaved surfaces, there are no extrinsic disorder effects induced by scraping.

It is worth comparing Ti_4O_7 in the HI phase with Fe_3O_4 above $T_V \simeq 120$ K because of the analogy between the two materials pointed out repeatedly [12]. For this purpose, we reanalyzed the PES spectra of Fe_3O_4 reported by Chainani *et al.* [14] in the context of an SCG. Figure 3 (a) shows the PES spectra of Fe_3O_4 measured with the resolution of ~ 70 meV. They claimed that the intensity at E_F in the metallic phase evolves as the temperature increases. In Fig. 3 (b), we have replotted the spectra against $E_B^2 \text{sgn}(E_B)$, which makes their argument clearer. More interestingly, we find that the 140 K ($> T_V$) spectrum almost falls on a straight line at $E_B \gtrsim 0.07$ eV. In contrast, the 100 K spectrum is slightly concave, signaling the opening of a hard gap. Fe_3O_4 is, however, different from Ti_4O_7 in that the 140 K spectrum, which would correspond to the HI-phase spectra of Ti_4O_7 , does not vanish at E_F but shows a finite Fermi edge. We have modeled the spectra $I(E_B, T)$ above T_V as $I(E_B, T) = I_0(E_B, T) + I_{bg}(E_B)$, where $I_0(E_B, T) = (a_2 E_B^2 + a_0)f(E_B, T)$ (a_0 : finite DOS at E_F). The 100 K spectrum was assumed to be $I_0(E_B, T) = a_2(E_B - E_0)^2 \theta(E_B - E_0)$ as in the LI phase of Ti_4O_7 . $I_{bg}(E_B) = b_1 E_B + b_0$ represents the linear background of the PES spectra [18]. The instrumental resolution was also included.

The result of the fitting was satisfying between $E_B = -0.15$ eV and 0.15 eV as shown by solid curves in Figs. 3 (a) and (b). The dashed curves in Fig. 3 (a) for $T \geq 140$ K represent the intrinsic DOS cut-off at E_F ($a_2 E_B^2 + a_0$) $f(E_B, 0)$. The most remarkable point is that the finite intensity at E_F evolves systematically with increasing temperature. Figure 3 (c) shows the ratio a_0/a_2 between the intensity at E_F , which contributes to the “metallic” conductivity, and the magnitude of the E_B^2 term, which represents the dynamical disorder. The electrical dc conductivity data of Fe_3O_4 [19] is superimposed in the figure. The a_0/a_2 values at 140, 200, and 300 K form a straight line which extrapolates to 0 at 119 ± 5 K $\sim T_V$. This observation, namely, $a_0/a_2 \propto T - T_V$ strongly indicates that $I_0 \propto E_B^2$ just above T_V . As the temperature goes up above T_V , the finite intensity at E_F grows up in proportion to $T - T_V$. Park *et al.* [20] reported that the spectra of Fe_3O_4 at 130 K show no Fermi edge, which is naturally understood as due to the small a_0/a_2 . We propose that an SCG exists in Fe_3O_4 just above T_V and continuously evolves into a pseudogap well above T_V , reflect-

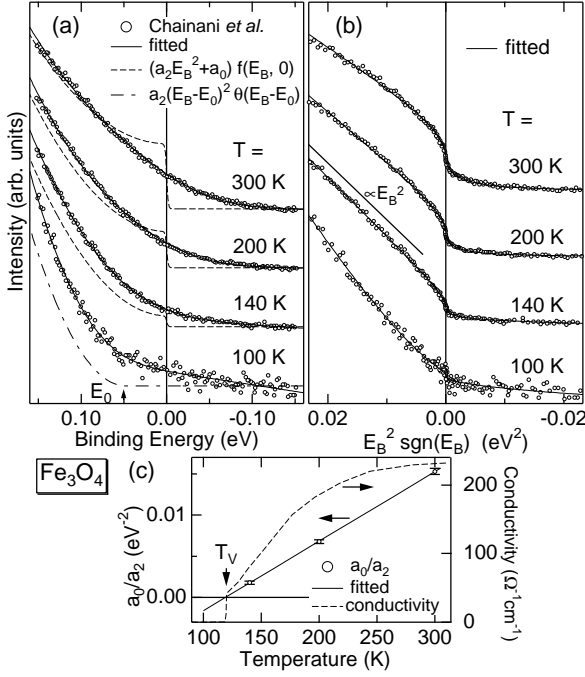


FIG. 3. (a) PES spectra of Fe₃O₄ ($h\nu = 21.2$ eV) taken from Ref. [14]. Solid, dashed, and dotted-dashed curves represent the fitted curves, $(a_2 E_B^2 + a_0)f(E_B, 0)$, and $a_2(E_B - E_0)^2 \theta(E_B - E_0)$, respectively. (b) The same spectra plotted against $E_B^2 \text{sgn}(E_B)$. (c) Ratio a_0/a_2 , which tends to vanish at $T \sim T_V$ (see text). The electrical conductivity of Fe₃O₄ is also shown by a dashed line [19].

ing the crossover from the semiconducting ($d\rho/dT < 0$) behavior just above T_V to the metallic ($d\rho/dT > 0$) one well above T_V . Just above T_V , charges are disordered with SRO, namely, the system is in a Wigner glass state [1] as is the HI phase of Ti₄O₇. Here, it should be noted that the M-phase spectra of Ti₄O₇ near E_F ($E_B < 0.2$ eV) may be fitted to $(a_2 E_B^2 + a_0)f(E_B, T)$ like the spectra of Fe₃O₄ above T_V . However, $a_0/a_2 = 2-4 \times 10^{-2}$ eV⁻² is much larger than that in Fe₃O₄ at 300 K, reflecting the strongly first-order transition between the HI and M phases in Ti₄O₇.

In conclusion, we have performed a PES study of Ti₄O₇ covering its LI, HI, and M phases. The spectra of the Ti 3d band show peculiar temperature-dependent spectra characteristic of the three phases, among which the HI-phase spectra are gapless and can be fitted to E_B^2 near E_F . We interpret this as an SCG resulting from disordered bipolarons. By reanalyzing the PES spectra of Fe₃O₄, an SCG was also found just above T_V , indicating the significant role of disorder and long-range Coulomb interaction. With increasing temperature, the SCG is found to continuously evolve into a pseudogap as the metallicity is gradually established, whereas the first-order HI-to-M transition in Ti₄O₇ precludes the observation of the corresponding continuous change. Presumably, similar SCG behavior may be observed in other

systems such as $\beta\text{-Na}_x\text{V}_2\text{O}_5$ [7]. The very recent scanning tunneling spectra of hole-doped manganites above T_C [21] may be interpreted in the same way as Fe₃O₄ above T_V .

We would like to thank D. Khomskii, M. Abbate, and T. Mizokawa for informative discussions. We appreciate Y. Aiura, K. Tobe and Y. Ishikawa for technical support. This work was supported by the New Energy and Industrial Technology Development Organization (NEDO) and by a Special Coordination Fund from the Science and Technology Agency of Japan.

* Present Address: Institute for Solid State Physics, University of Tokyo, Tokyo 106-8666, Japan.

- [1] N. F. Mott, *Metal-Insulator Transitions* (Taylor & Francis, London, 1990).
- [2] P. W. Anderson, Phys. Rev. Lett. **34**, 953 (1975).
- [3] A. L. Efros and B. I. Shklovskii, J. Phys. C **8**, L49 (1975).
- [4] J. G. Massey and M. Lee, Phys. Rev. Lett. **77**, 3399 (1996); **75**, 4266 (1995).
- [5] J. H. Davies and J. R. Franz, Phys. Rev. Lett. **57**, 475 (1986).
- [6] G. Hollinger *et al.*, Phys. Rev. B **32**, 1987 (1985); M. D. Hill and R. G. Egdell, J. Phys. C **16**, 6205 (1983).
- [7] C. Schlenker, *Physics of Disordered Materials*, eds. by D. Alder, H. Fritzschke, and S. Ovshinsky (Plenum, New York, 1985) p. 369.
- [8] M. Marezio *et al.*, Phys. Rev. Lett. **28**, 1390 (1972).
- [9] C. Schlenker *et al.*, Phys. Rev. Lett. **32**, 1318 (1974).
- [10] S. Lakkis *et al.*, Phys. Rev. B **14**, 1429 (1976).
- [11] C. Schlenker and M. Marezio, Philos. Mag. B **42**, 453 (1980).
- [12] B. K. Chakraverty, Philos. Mag. B **42**, 473 (1980).
- [13] E. J. W. Verwey and P. W. Haaymann, Physica **8**, 979 (1941).
- [14] A. Chainani *et al.*, Phys. Rev. B **51**, 17976 (1995).
- [15] J. J. Since, S. Ahmed, and J. Mercier, J. Crystal Growth **40**, 301 (1977).
- [16] M. Abbate *et al.*, Phys. Rev. B **51**, 10150 (1995).
- [17] A. Fujimori *et al.*, Phys. Rev. Lett. **69**, 1796 (1992); I. H. Inoue *et al.*, *ibid.* **74**, 2539 (1995).
- [18] Because of the very low intrinsic photoemission signals around E_F for Fe₃O₄, the linear background due to satellites ($h\nu = 23-24$ eV) of the He I light had to be taken into account. Unlike Fe₃O₄, the satellites are negligibly weak in the spectra of Ti₄O₇ around E_F .
- [19] S.-K. Park, T. Ishikawa, and Y. Tokura, Phys. Rev. B **58**, 3717 (1998).
- [20] J.-H. Park *et al.*, Phys. Rev. B **55**, 12813 (1997).
- [21] A. Biswas *et al.*, Phys. Rev. B **59**, 5368 (1999).